The Benzodiphosphaalkene Ligand and Its Pd^{II} and Pt^{II} Complexes: Their Synthesis, Structure, and an ESR Study of Their Reduction Products

Abdelaziz Jouaiti,[†] Michel Geoffroy,*[,†] Gustavo Terron,[†] and Gérald Bernardinelli[‡]

Contribution from the Department of Physical Chemistry, 30 Quai Ernest Ansermet, University of Geneva, Geneva, Switzerland, and Laboratory of Crystallography, 24 Quai Ernest Ansermet, University of Geneva, Geneva, Switzerland

Received June 24, 1994[⊗]

Abstract: The new diphosphaalkene 1,3-bis[2-(2,4,6-tri-*tert*-butylphenyl)phosphanediylmethyl]benzene, **L**, has been synthesized. Due to the presence of two P=C bonds three isomers (EE, EZ, ZZ) were observed by ^{31}P NMR, and the crystal structures of two of them could be determined (EE, ZZ). The electrochemical behavior of **L** has been studied by cyclic voltametry: a quasi-reversible reduction occurs at −1.89 V/SCE and corresponds to the formation of a radical anion which has been studied by ESR at variable temperature. The experimental ^{31}P and ^{1}H hyperfine constants are consistent with free rotation about the P=C and $C_{phosphaalkene}$−$C_{benzene}$ bonds at room temperature and agree with *ab initio* predictions. One of the isomers of **L** forms complexes with palladium(II) and platinum(II) ions. The crystal structures show that **L** is orthometalated and acts as a terdentate ligand by coordinating the metal with each phosphorus atom. These complexes are electrochemically reduced between −0.92 and −1.29 V, and the resulting paramagnetic species are studied by ESR in liquid and frozen solutions. This reduction process was shown to be a ligand-centered process, an appreciable part of the unpaired electron is localized on each of the phosphaalkene carbons (20%) and phosphorus atoms (5%).

Introduction

Chelating agents have long been used in almost all branches of chemistry to extract metal ions from solutions, but it has been realized only within the last few years that the resulting metallic complexes can exhibit particularly interesting physicochemical properties[1−7] and that they can be used as "building blocks" in supramolecular chemistry. Furthermore, some of these compounds present interesting photosensitizer properties. This is the case, for example, for tris(α-diiimineruthenium)[8,9] complexes which, in their metal-to-ligand charge transfer (MLCT) excited state, accommodate an unpaired electron in a π^* orbital of the ligand. Terdentate monoanionic aryl ligands like 2,6[Me_2NCH_2]$_2C_6H_3$—the pincer ligand[10] —have been shown to stabilize and control metal centered reactions. Moreover, with molecules like 1,3-di-*o*-pyridylbenzene,[11,12] it has recently been shown that orthometallation provides excellent communication to the molecule when used as a bridging ligand.

While the −P=C< group is well-known for its coordination properties, until our preliminary communication,[13] terdentate ligands in which the chelating functions were ensured by several phosphaalkene groups and cyclometallation had not yet been reported. However, the ability of dicoordinated trivalent phosphorus to form η^1 bonds[14−16] appears appropriate for the formation of new chelates and, for example, **L** is expected to act as a terdentate ligand for metals which are likely to give rise to orthometallation (**LMX**).

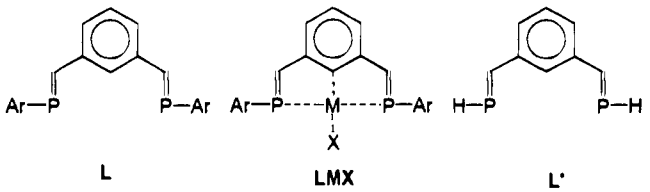

Ar: $C_6H_2{}^tBu_3$-2,4,6

In the resulting complex the separation between the ligand π^* orbital and the metal d_π orbitals is probably small and the excess electrons resulting from a reduction process could be largely shared by the metal and the ligand.

In the present study, we report the synthesis of **L** as well as a study of its electrochemical behavior. Since various orienta-

[†] Department of Physical Chemistry.
[‡] Laboratory of Crystallography.
[⊗] Abstract published in *Advance ACS Abstracts*, February 1, 1995.

(1) , Lehn, J.-M.; Rigault, A. *Angew. Chem., Int. Ed. Engl.* **1988**, *27*, 1095.
(2) Baxter, P.; Lehn, J.-M.; DeCian, A.; Fisher, J. *Angew. Chem., Int. Ed. Engl.* **1993**, *32*, 69.
(3) Serroni, S.; Denti, G.; Campagna, S.; Ciano, M.; Balzani, V. *J. Chem. Soc., Chem. Commun.* **1991**, 944.
(4) Denti, G.; Campagna, S.; Serroni, S.; Ciano, M.; Balzani, V. *J. Am. Chem. Soc.* **1992**, *114*, 2944.
(5) Williams, A. F.; Piguet, C.; Bernardinelli, G. *Angew. Chem., Int. Ed. Engl.* **1991**, *30*, 1490.
(6) Sauvage, J.-P. *Acc. Chem. Res.* **1990**, 23, 319.
(7) Dietrich-Brücheker, C. O.; Guilhem, J.; Pascard, C.; Sauvage J.-P. *Angew. Chem., Int. Ed. Engl.* **1990**, *29*, 1154.
(8) Kaim, W.; Ernst, S.; Kohlmann, S.; Welkerling, P. *Chem. Phys. Lett.* **1985**, *118*, 431.
(9) Kaim, W.; Ernst, S.; Kasack, V. *J. Am. Chem. Soc.* **1990**, *112*, 173.
(10) Grove, D. M.; Van Koten, G.; Louwen, J. N.; Noltes, J. G.; Spek, A. L.; Ubbels, H. J. C. *J. Am. Chem. Soc.* **1982**, *104*, 6609.
(11) Beley, M.; Collin, J.-P.; Louis, R.; Metz, B.; Sauvage, J.-P. *J. Am. Chem. Soc.* **1991**, *113*, 8521.
(12) Beley, M.; Collin, J.-P.; Sauvage, J.-P. *Inorg. Chem.* **1993**, *32*, 4539.
(13) Jouaiti, A.; Geoffroy, M.; Terron, G.; Bernardinelli, G. *J. Chem. Soc., Chem. Commun.* **1992**, 155.
(14) Klebach, Th. C.; Lourens, R.; Bickelhaupt, F.; Stam, C. H.; Van Herk, A. *J. Organomet. Chem.* **1981**, *210*, 211.
(15) Eshtiagh-Hosseini, H.; Kroto, H. W.; Nixon, J.-F.; Maah, M. J.; Taylor, M. J. *J. Chem. Soc. Chem. Commun.* **1981**, 199.
(16) Van der Knaap, Th. A.; Bickelhaupt, F. *J. Am. Chem. Soc.* **1982**, *104*, 1756.

0002-7863/95/1517-2251$09.00/0 © 1995 American Chemical Society

tions of the central phenyl ring and of the two phosphaalkene groups are possible in this molecule, **L** is expected to adopt a large number of conformations. We could, indeed, crystallize two of these rotamers, and their structures will be described here. After electrochemical reduction, liquid and solid state ESR spectra of **L** yield a hyperfine structure that reveals that rapid exchange between several conformers probably occurs at room temperature. The experimental spin delocalization will be compared with the spin densities predicted by *ab initio* calculations for the model diphosphaalkene radical anion $\mathbf{L'}^{-}$.

Evidence of the ability of **L** to chelate transition metal ions is obtained from the crystal structure of its palladium and platinum complexes. These complexes are easily reduced, and information about the delocalization of the additional electrons is obtained from ESR spectra.

Experimental Section

Equipment and Methods. NMR spectra were recorded on a Bruker AC-200F (^{1}H, 200 MHz; ^{31}P, 81 MHz) spectrometer. External H_3PO_4 was used as reference. Electrochemical measurements were carried out at room temperature by using a Princeton Applied Research scanning potentiostat (Model 362). Cyclic voltamograms were obtained in acetonitrile or THF solutions by using a platinum electrode and a SCE reference electrode with tetrabutylammonium hexafluorophosphate as supporting electrolyte. Under the conditions used, the redox potential of the fc/fc$^+$ couple was $E^1/_2 = 0.56$ V in THF.

The ESR spectra were obtained on a Bruker 200D spectrometer (100 kHz field modulation, X-band) equipped with a VT1100 variable temperature controller. The paramagnetic species were generated by *in situ* electrolysis using a homemade quartz cell (Pt electrodes and Ag/Hg reference electrode). The frozen solution spectra were simulated by using a program which generates the envelope resulting from 120 000 random orientations of the magnetic field. An additional subroutine (simplex algorithm) enabled us to optimize the ESR tensors when the same line width could be used for all the transitions of the spectrum. The contribution of each orientation was calculated with second-order perturbation[17] by using a Hamiltonian which takes the electronic Zeeman effect and the hyperfine couplings into account.

Ab initio calculations were carried out on a Silicon Graphics computer (IRIS 4D) by using the Gaussian 90 program[18] and, in general, the 6-31G* basis set. Due to the large size of the molecule **L**, the calculations were carried out on the molecule **L'**. All the results reported here were obtained by using the ROHF method (UHF calculations performed on $\mathbf{L'}^{-}$ led to $\langle S^2 \rangle$ values greater than 0.75).

X-ray Crystallography. Cell dimensions and intensities were measured at room temperature on a Philips PW1100 diffractometer for the EE and ZZ compounds with graphite-monochromated Mo Kα radiation (λ = 0.710 69 Å) and at 180 K on a Nonius CAD4 diffractometer with graphite-monochromated Cu Kα radiation (λ = 1.5418 Å) for the Pt complex. Two reference reflections measured every 60 min showed a decrease of about 39% for the EE and 9% for the ZZ compounds; all intensities were corrected for these drifts. Data were corrected for Lorentz and polarization effects and for absorption[19] (Pt complex). The structures were solved by direct methods using MULTAN 87,[20] all other calculations used the XTAL[21] system and ORTEP[22] programs. Atomic scattering factors and anomalous dispersion terms were taken from ref 23. All coordinates of the hydrogen atoms have been calculated. It should be noted that the relatively large *R* values reported below for the three crystal structures are essentialy due to (1) partial decomposition of the compounds under X-ray exposure, (2) large values of atomic displacement parameters due to presence of *t*-butyl substituents (low density compounds), and (3) presence of solvent of inclusion for the Pt complex. For both E_1E_1 and Z_1Z_2 compounds, refinements have been performed with unit weighting schemes in order to avoid physically unreasonable anisotropic displacement parameters.

Syntheses. Most of the syntheses were performed under argon atmosphere in carefully dried glassware. All the reagents were purchased from Fluka and used as received. $ArPH_2$,[24] $Pd(NCPh)_2Cl_2$,[25] and $Pt(NCCH_3)_2Cl_2$[26] were synthesized according to previously reported procedures.

1. **Preparation of the Ligands. A. Isomers EE and EZ.** The phosphaalkene group was generated following the method of Yoshifuji et al.[27] A 3.23-mL (5 mmol) portion of a solution (1.6 M) of *n*-BuLi in hexane was added at room temperature to a carefully degassed solution containing 1.44 g (5 mmol) of $ArPH_2$ in freshly distilled THF. Then 0.78 g (5 mmol) of ^{t}BuMe$_2$SiCl was added all at once to the solution and an equivalent of *n*-BuLi was added to the mixture. The resulting solution was stirred for 5 min at room temperature, and 0.335 g (2.5 mmol) of isophthalaldehyde was added. The solution was stirred for 2 h and evaporated to dryness. The two isomers EE and EZ (15%) were purified on a column using pentane as an eluant (yield 60%, 0.92 g). They were then recrystallized from an ether/acetonitrile solution.

Analytical data: Isomer EE, mp, 148−150 °C; ^{31}P {^{1}H} NMR ($CDCl_3$) δ 261.71 (s, 2P) ppm; ^{1}H NMR ($CDCl_3$) 1.42 (s, 18H, *p*-^{t}Bu), 1.50 (s, 36H, *o*-^{t}Bu), 7.30 (t, 1H, ^3J = 7 Hz, H(5)), 7.51 (s, 4H, Ar−*H*), 7.60 (m, 3H, central phenyl), 8.17 (d, 2H, $^2J_{H-P}$ = 23.5 Hz, *H*−C=P) ppm. Isomer EZ, mp, 120−122 °C; ^{31}P {^{1}H} NMR ($CDCl_3$) δ 259.72 (s, 1P, P(1)), 242.51 (s, 1P, P(2)) ppm; ^{1}H NMR ($CDCl_3$) δ 1.42 (s, 9H, *p*-^{t}Bu), 1.38 (s, 9H, *p*-^{t}Bu), 1.49 (s,18H, *o*-^{t}Bu), 1.46 (s, 18H, *o*-^{t}Bu), 6.22 (m, 2H, H(6), (4)), 6.94 (t, 1H, ^3J = 7 Hz, H(5)), 7.39 (d, 2H, J = 0.95 Hz, Ar−*H*), 7.45 (s, 2H, Ar−*H*), 7.56 (m, 1H, H(2)), 7.70 (d,1H, $^2J_{H-P}$ = 25.55 Hz, H(7)), 7.80 (d, 1H, $^2J_{H-P}$ = 38.09 Hz, H(8)) ppm.

Deuteration of Isomer EE. Deuterated isophthalaldehyde was used as a reagent. This latter compound was synthesized by treating $C_6H_4(C(O)OCH_3)_2$ with $LiAlD_4$ in THF and by oxidizing the resulting $C_6H_4(CD_2OD)_2$ with MnO_2.

2. Preparation of the Complexes. A. LPdCl. A 58-mg (0.15 mmol) portion of $(PhCN)_2PdCl_2$ was added all at once to a solution of 100 mg (0.15 mmol) of **L** in 5 mL of CH_2Cl_2. The orange mixture was stirred for 2 h at room temperature. Then 3 mL of benzene or EtOH was added. Orange crystals of LPdCl were grown after slow evaporation of the solution under argon atmosphere.

Analytical data: mp = 181 °C (dec); ^{31}P {^{1}H} NMR ($CDCl_3$) δ 227.12 (s, 2P) ppm; ^{1}H NMR ($CDCl_3$) δ 1.35 (s, 18H, *p*-^{t}Bu), 1.70 (s, 36H, *o*-^{t}Bu), 6.85 (m, 2H, H(4),(6)), 6.92 (m, 1H, H(5)), 7.52 (t, 4H, J = 2 Hz, Ar−*H*), 7.61 (t, 2H, $|^2J_{H-P} + {}^4J_{H-P}|$ = 17 Hz, *H*−C=P) ppm.

B. [LPd NCCH$_3$]$^+$BF$_4^-$. A 67-mg (0.15 mmol) portion of $[(CH_3CN)_4Pd]^{2+}[BF_4^-]_2$ was added all at once to a solution of 100 mg (0.15 mmol) of **L** in 5 mL of CH_2Cl_2. The mixture was stirred at room temperature for 2 h. The solvent was removed, and the residue was dissolved in a minimum quantity of ethanol. Orange crystals were obtained at −5 °C.

(17) Iwasaki, M. *J. Magn. Reson.* **1974**, *16*, 417.

(18) Frisch, F. M. J.; Head-Gordon, M.; Trucks, G. W.; Foresman, J. B.; Schlegel, H. B.; Raghavachari, K.; Robb, M.; Binkley, J. S.; Gonzalez, C.; Defrees, D. J.; Fox, D. J.; Whiteside, R. A.; Seeger, R.; Melius, C. F.; Baker, J.; Martin, R. L.; Kahn, L. R.; Stewart, J. J. P.; Topiol, S.; Pople, J. A. *Gaussian 90*; Gaussian, Inc.: Pittsburgh, PA, 1990.

(19) Blanc, E.; Schwarzenbach, D.; Flack, H. D. *J. Appl. Crystallogr.* **1991**, *24*, 1035.

(20) Main, P.; Fiske, S. J.; Hull, S. E.; Lessinger, L.; Germain, G.; Declercq, J.-P.; Woolfson, M. M. *A System of Computer Programs for the Automatic Solution of Crystal Structures from X-Ray Diffraction Data*; University of York and Louvain-la-Neuve: York, England, and Louvain, Belgium, 1987.

(21) Hall, S. R.; Flack, H. D.; Stewart, J. M. *Eds XTAL3.2 User's Manual*; Universities of Western Australia and Maryland: Australia and Maryland, 1992.

(22) Johnson, C. K. ORTEP II. Report ORNL-5138; Oak Ridge National Laboratory: Oak Ridge, TN, 1976.

(23) *International Tables for X-ray Crystallography*; Hilbers, J. A., Hamilton, W. C., Eds.; Kynoch: Birmingham, 1974; Vol. IV.

(24) Cowley, A. H.; Kilduff, J. E.; Lasch, J. G.; Mehrotra, S. K.; Norman, N. C.; Pakulski, M.; Whittlesey, B. R.; Atwood, J. L.; Hunter, W. E. *Inorg. Chem.* **1984**, *23*, 2582.

(25) Doyle, J. R.; Slade P. E.; Jonassen, H. B. *Inorg. Synth.* **1960**, *6*, 218.

(26) Hartley, F. R.; Murray, S. G.; McAuliffe, C. A. *Inorg. Chem.* **1979**, 18, 1394.

(27) Joshifuji, M.; Toyota, K.; Inamoto, N. *Tetrahedron Lett.* **1985**, 26, 1727.

Analytical data: $^{31}P\{^1H\}$ NMR ($CDCl_3$) δ 222.33 (s, 2P) ppm; ^1H NMR ($CDCl_3$) 1.37 (s, 18H, *p*-^{t}Bu), 1.68 (s, 36H, *o*-^{t}Bu), 6.8 (m, 2H, H(4), (6)), 6.85 (m, 1H, H(5)), 7.58 (t, 4H, J = 2 Hz, Ar−*H*), 7.63 (t, 2H, $|^2J_{H-P} + {}^4J_{H-P}|$ = 16 Hz, *H*−C=P) ppm.

C. LPtCl. A 52-mg (0.15 mmol) portion of $(CH_3CN)_2PtCl_2$ was added to a solution containing 100 mg (0.15 mmol) of **L** in 10 mL of $CHCH_3$. The resulting solution was heated at reflux during 36 h. The solvent was removed by rotatory evaporation, and the remaining solid was separated by "flash" chromatography on a silica gel column using hexane/CH_2Cl_2 as an eluant. Slow evaporation of the orange fraction afforded dark orange needles (mp 226 °C).

Analytical data: $^{31}P\{^1H\}$ NMR ($CDCl_3$) δ 211.24 (s+d, 2P, $^1J_{P-^{195}Pt}$ = 3998.13 Hz) ppm; ^1H NMR ($CDCl_3$) δ 1.36 (s, 18H, *p*-^{t}Bu), 1.71 (s, 36H, *o*-^{t}Bu), 6.93 (m, 1H, H(5)), 7.02 (m, 2H, H(4), (6)), 7.56 (t, 4H, J = 2 Hz, Ar−*H*), 7.88 (t + dt, 2H, $|^2J_{H-P} + {}^4J_{H-P}|$ = 10 Hz, $^3J_{H-^{195}Pt}$ = 45 MHz, *H*−C=P).

Crystal Structure Analysis of the E_1E_1 Compound. $C_{44}H_{64}P_2$, M_r = 654.9; μ(Mo Kα) = 0.124 mm^{-1}, $F(000)$ = 1432, d_x = 1.02 g·cm^{-3}, monoclinic, $P2_1/c$, Z = 4, a = 16.507(2), b = 13.800(2), c = 20.403(3) Å, β = 113.90(1)°, V = 4249(1) Å^3, from 30 reflections (14° < 2θ < 23°), pale yellow prism 0.18 × 0.20 × 0.25 mm mounted on a quartz fiber, −16 < h <16; 0 < k < 14; 0 < l < 20; 298 K; 5152 unique reflections measured of which 2505 were observable ($|F_o| > 4\sigma(F_o)$). Full-matrix least-squares refinement based on F using weight of 1 gave final values $R = \omega R$ = 0.091 and S = 3.55 for 415 variables. The maximum shift/error on the last cycle was 0.015. The final difference electron density map showed a maximum of +0.58 and a minimum of −0.67 e Å^{-3}. It should be noted that although the metric of the unit cell parameters is orthorhombic (CREDUC[28]), the symmetry of the diffracted intensities is consistent with a monoclinic system. Moreover, an investigation of the atomic coordinates with the program MISSYM[29] does not indicate a supplementary symmetry element.

Crystal Structure Analysis of the Z_1Z_2 Compound. $C_{44}H_{64}P_2$, M_r = 654.9; μ(Mo Kα) = 0.128 mm^{-1}, $F(000)$ = 716, d_x = 1.06 g cm^{-3}, triclinic, $P\bar{1}$, Z = 2, a = 10.700(3), b = 13.882(4), c = 14.223(3) Å, α = 90.74(1), β = 95.50(2), γ = 101.77(2)°, V = 2058(1) Å^3, from 25 reflections (15° < 2θ < 24°), colorless prism, 0.10 × 0.15 × 0.20 mm mounted on a quartz fiber, −10 < h <10; −13 < k < 13; 0 < l < 13; 298 K; 3814 unique reflections measured of which 1941 were observable ($|F_o| > 4\sigma(F_o)$). Full-matrix least-squares refinement based on F using weight of 1 gave final values $R = \omega R$ = 0.093 and S = 2.82 for 415 variables. The maximum shift/error on the last cycle was 0.011. The final difference electron density map showed a maximum of +0.63 and a minimum of −0.68 e Å^{-3}.

Crystal Structure Analysis of the LPtCl Complex. PtCl-($C_{44}H_{63}P_2$)(CH_2Cl_2), M_r = 969.4; μ(Cu Kα) = 8.456 mm^{-1}, A^* min, max = 2.54, 7.95; $F(000)$ = 1976, d_x = 1.43 g·cm^{-3}, monoclinic, $P2_1/n$, Z = 4, a = 9.381(2), b = 33.792(6), c = 14.796(3) Å, β = 106.077(6)°, V = 4507(2) Å^3, from 24 reflections (44° < 2θ < 62°), red prism, 0.16 × 0.18 × 0.30 mm mounted in a Lindemann capillary, −9 < h < 9; 0 < k < 32; 0 < l < 14; 180 K; 4421 unique reflections measured of which 3649 were observables ($|F_o| > 4\sigma(F_o)$). Full-matrix least-squares refinement based on F using weight of $1/\sigma^2(F_o)$ gave final values $R = \omega R$ = 0.060 and S = 6.22 for 460 variables. The maximum shift/error on the last cycle was 0.021. The final difference electron density map showed maximum and minimum of +2.31 and −2.42 e Å^{-3} about the Pt atom.

Results

For the molecules **L** or **L′** with their P=C bonds in the plane of the phenyl ring, the presence of the two phosphaethylene bonds generates three rotamers: EE, EZ (identical to ZE), and ZZ. Furthermore, each of these rotamers gives rise to four isomers characterized by their C(2)−C(1)−C(7)−P and C(2)−C(3)−C(8)−P dihedral angles (β1 and β2, repectively) which can be close to 0° (isomer referred by subscript 1) or to 180° (isomer referred by subscript 2). Some examples are given in Figure 1 for **L′**.

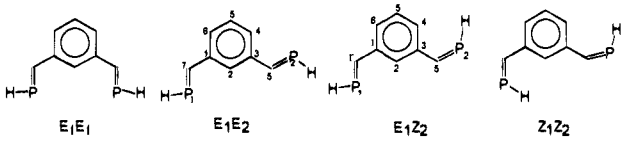

Figure 1. Examples of isomers for **L′**.

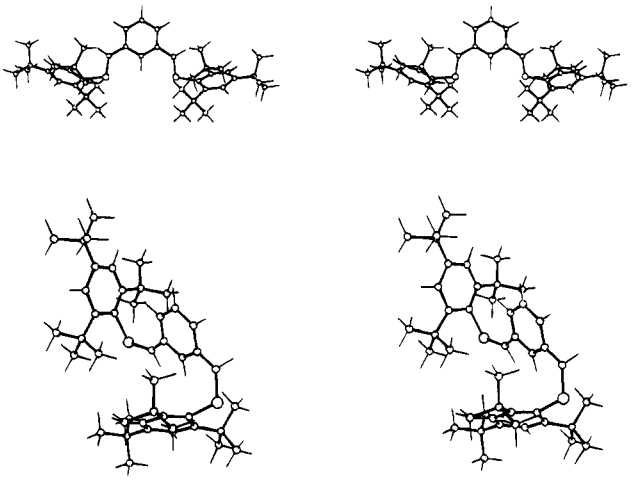

Figure 2. Crystal structures of the E_1E_1 (top) and Z_1Z_2 (bottom) isomers of **L**.

Two isomers of **L** have been isolated and have been easily distinguished by their ^{31}P NMR spectrum: the EZ isomer which exhibits two ^{31}P resonances at δ = 259.7 ppm and δ = 242.5 ppm and the EE isomer, identified from its crystal structure (*vide infra*), which exhibits a single ^{31}P resonance at δ = 261.71 ppm. When a solution containing these isomers was stored for 1 day, without any protection from light, an additional signal, undoubtedly due to the formation of the ZZ isomer, appeared at 242 ppm in the ^{31}P NMR spectrum. Exposure of a benzene solution of **L** to UV/vis light induces, indeed, the isomerization of the EE form into the EZ and ZZ conformers.[30] Single crystals of the EE isomer, suitable for crystal structure determination by X-ray diffraction, could be obtained from a solution in benzene/acetonitrile. However, solutions of the EZ isomer led to an amorphous compound. It was nevertheless possible to grow some crystals after a very slow evaporation (several weeks) at −25 °C of a solution containing the EZ isomer in an ether/acetonitrile mixture. However, as described below, this crystal was in fact the ZZ isomer which probably resulted from a slow transformation of EZ. The crystal structures of the E_1E_1 and Z_1Z_2 isomers are described below, together with those of the platinum and palladium[13] complexes.

Crystal Structures. The atom numbering refers to Figure 1. Stereoviews for the E_1E_1 and Z_1Z_2 isomers of **L** are shown in the top and bottom portions of Figure 2, respectively. For these structures the aromatic rings show no major distortion from planarity, and the P=C bond lengths (mean value 1.667 Å) are comparable to those already reported for the monophosphaalkenes.[31] While the phosphorous atoms are almost coplanar with the central benzene ring (see the C(2)−C(1)−C(7)−P(1) and C(2)−C(3)−C(8)−P(2) dihedral angles in Table 1) in the **LMCl** complexes, the EE and ZZ isomers of **L** show some

(28) Le Page, Y. *J. Appl. Crystallogr.* **1982**, 15, 255.
(29) Le Page, Y. *J. Appl. Crystallogr.* **1987**, 20, 264.

(30) When a solution containing 74% EE, 20% EZ, and 6% ZZ was photolyzed for 1 h with 320 nm radiation, its composition changed to: EE, 42%; EZ, 46%; ZZ, 12%. (λ = 320 nm corresponds to an intense absorption band of the EE isomer.) By use of the nonfiltrated radiation of a high pressure Hg lamp (Osram 500 W) a solution composed of EE (87%), EZ (11%), and ZZ (2%) transformed into a solution of composed of EE (20%), EZ (40%), and ZZ (40%) after 5 h irradiation.

(31) Appel, R.; Menzel, J.; Knoch, F.; Volz, P. *Z. Anorg. Chem.* **1986**, *534*, 100.

Table 1. Selected Bond Lengths (Å), Bond Angles, and Torsional Angles (deg) for EE and ZZ Isomers of **L** and for **LPtCl** and **LPdCl**

	L(E1E1)	L(Z1Z2)	LPtCl	LPdCl[a,13]
M−P(1)			2.259(4)	2.274(3)
M−P(2)			2.263(4)	2.274(3)
M−C(2)			2.06(1)	2.04(1)
P···P	5.467(6)	7.355(6)	4.465(5)	4.490(5)
C(9)−P(1)−C(7)[b]	101.1(6)	107.1(7)	113.3(7)	111.3(5)
P(1)−C(7)−C(1)	125(1)	134(1)	114(1)	116.1(6)
C(3)−C(8)−P(2)	125.3(7)	139(1)	115(1)	116.1(8)
C(8)−P(2)−C(15)[b]	100.4(5)	107.3(7)	113.2(7)	111.3(5)
C(2)−C(1)−C(7)−P(1)	24(2)	−32(3)	0(2)	0(1)
C(2)−C(3)−C(8)−P(2)	13.2	170(1)	−2(2)	0(1)
C(1)−C(7)−P(1)−C(9)[b]	−179(1)	5(2)	179(1)	178.2(8)
C(3)−C(8)−P(2)−C(15)[b]	180(1)	0(2)	−168(1)	178.2(8)
ξ[c]	62.1; 66.7	81.2; 57.7	89.2; 85.9	86.0, 86.0

[a] LPdCl is located on a special position with the Pd, Cl, C(2), and C(5) atoms on a C_2-axis. [b] C(9) and C(15) correspond to the carbon of the Ar groups which are bound to P(1) and P(2), respectively. [c] ξ is the dihedral angle between the mean plane of the central benzene ring and an Ar group.

Table 2. Electrochemistry of the Diphosphaalkene Ligand **L** and its Metal Complexes[a]

	$E^1/_2$ (ΔEp)[b]		
compound	II/I state	I/0 state	0/−I state
L (isomer EE)[c]			−1.89 (130)
L (isomer EZ)[c]			−1.89 (130)
ArP=C(H)Ph (isomer E)[32]			−1.98 (339)
LPdCl[c]	−1.23 (110)	−1.92[d]	
LPdNCMe$^+$[c]	−0.92 (80)	−1.6[d]	
LPtCl[c]	−1.29 (80)	−1.94[d]	

[a] Conditions: THF, 0.1M n-Bu_4PF_6, Pt as working electrode. [b] Volts vs SCE reference $E^1/_2$ in V, ΔE in mV. [c] Scan rates: 10 mV/s, except for LPdCl: 50 mV/s. [d] Irreversible.

distortion from planarity. This effect is more accentuated in the Z_1Z_2 isomer due to steric hindrance between the bulky substituted aryl groups and leads to a significant opening of the valence angles at the C(7) and C(8) atoms. The distortion around the P=C double bond is weak (deviations between 0 and 5°) except for one side of the Pt complex where the observed deviation was 12°. It should be noted that the presence of the metal and chlorine atoms precludes the rotation of the substituted aryl groups, which are oriented perpendicular to the central benzene ring, and leads to short steric interactions between the methyl groups of the tri-*tert*-butyl substituents. This situation constrains the complexes to adopt a pseudosymmetry (two mirror planes). For the two isomers of **L** and for both **LMCl** complexes, the angle formed by the plane of each Ar ring with the plane of the central benzene ring is rather large (superior to 57°) and suggests that no delocalization will be possible between these groups. Compared to the E_1E_1 free ligand, the P···P distance of the metal complexes is significantly shorter. Consequently, the bond angles at C(7) and C(8) are more closed.

Electrochemistry. Electrochemical data are given in Table 2. The fact that the peak current ratio (i_{pa}/i_{pc}) was less than unity and that ΔE_p increased with scan rate was indicative of a quasi-reversible process for the reduction of both ligand isomers and for the first reduction of the complexes. The reduction potential was the same for the EE and EZ compounds (−1.8 V) and was slightly higher than the potential found for the monophosphaethylene derivative (−1.9 V). For each palladium or platinum complex two reduction waves were detected; the first one was quasi-reversible and occurred approximately 0.60 V higher than the second reduction potential which corresponded to an irreversible process. No oxidation in THF could be observed for any investigated compound.

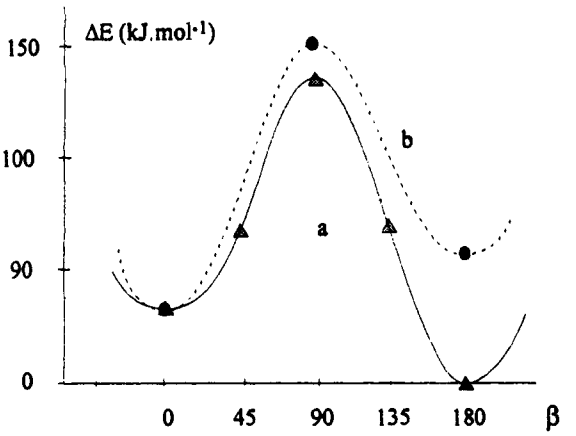

Figure 3. Variation of the energy of $\mathbf{L'}^-$ during the transformation $E_1E_1 \rightarrow E_2E_2$. In this transformation both dihedral angles C(2)−C(1)−C(7)−P and C(2)−C(3)−C(8)−P are equal (β angle). The curves a and b correspond to the ^{2}A and ^{2}B states, respectively.

Calculations. Optimization of geometries for the various isomers of $\mathbf{L'}^-$ was performed by assuming that (1) the benzene ring retains D_{6h} symmetry and (2) both phosphaalkene moieties have the same bond lengths and bond angles and that they differ only in their torsion angles. While reasonable wave functions were obtained for the isomers of C_{2v} symmetry, unstable wave functions leading to an artificial localization of the spin on a single phosphaalkene group were obtained for C_s structures. This is reminiscent of previous studies on symmetry-broken solutions found for open shell electronic states represented by more than one low energy structure in valence-bond descriptions.[33] Such a problem, which can be solved only by using a MCSCF approach, is beyond the scope of this experimental study, and for the present calculations, we will consider only the isomers of C_{2v} structure.

In order to estimate the energy barrier to the isomerization of E_1E_1 into E_2E_2, we have calculated the dependence of the energy of the radical ion upon the β_1 and β_2 dihedral angles. This dependence, shown in Figure 3, corresponds to a transformation which maintains β_1 equal to β_2 (C_2 and C_{2v} symmetries). The planar conformations correspond, indeed, to energy minima. It is worth mentioning that out of the two possible symmetries found for the singly occupied molecular orbital (SOMO) of the C_{2v} conformers (Figure 4), the $^2B_1$ state was found to be the more stable configuration only for the E_1E_1 isomer (Figure 3), but in this case the energy difference with the $^2A_2$ state was found to be only 0.4 kJ·mol^{-1}. In this paper,

(32) Geoffroy, M. ; Jouaiti, A.; Terron, G.; Cattani-Lorente, M.; Ellinger, Y. *J. Phys. Chem.* **1992**, *96*, 8241.

(33) McLean, A. D.; Lengsfield, B. H., III; Pacansky, J.; Ellinger, Y. *J. Chem. Phys.* **1985**, 87, 3567.

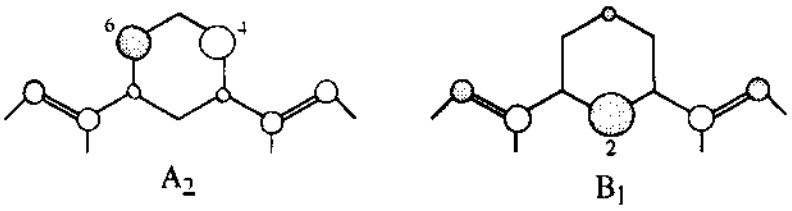

Figure 4. Representation of the SOMO for the A_2 and B_1 states.

Table 3. Energies and Spin Densities[a] for $\mathbf{L}^{\bullet-}$ Rotamers (C_{2v} Symmetry, $^2A_2$ State)

	E_1E_1	E_2E_2	Z_1Z_1	Z_2Z_2
E (hartree)	−988.952234	−988.964942	−988.964981	−988.964543
ϱC(2)	0.000	0.000 (0.000)	0.000	0.000
ϱC(4)	0.321	0.221 (0.214)	0.224	0.227
ϱC(5)	0.000	0.000 (0.000)	0.000	0.000
ϱC(6)	0.214	0.221 (0.214)	0.224	0.227
ϱC(7)	0.107	0.113 (0.009)	0.103	0.108
ϱP(1)	0.125	0.120 (0.150)	0.118	0.117
ϱC(8)	0.107	0.113 (0.009)	0.103	0.108
ϱP(2)	0.125	0.120 (0.150)	0.118	0.117

[a] Values given in parentheses have been obtained by using the 6.31++G** basis set. The other values have been obtained with the 6-31G* basis.

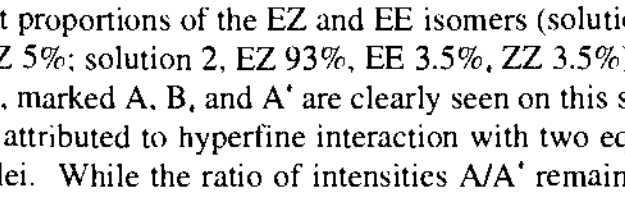

Figure 5. Definition of the ϕ angle for H_2PCH.

we will assume that the ground state of all the C_{2v} rotamers is the $^2A_2$ state; the corresponding spin densities calculated with the 6-31G* basis are shown in Table 3 together with the values obtained for the E_2E_2 isomer by using a 6.311^{++}G** basis set. This latter basis set, which incorporates diffuse functions, is particularly appropriate to the study of radical anions. It leads to spin densities which are similar to those obtained with the 6.31G* basis set which can therefore be considered as satisfactory.

In order to estimate the energy barrier through the P=C bond we have optimized several structures of the H_2C=PH molecule by using second-order Møller−Plesset[34] (MP2) calculations. For these optimizations, the H_2CP group was constrained to be planar, and the energy was calculated as a function of the ϕ dihedral angle (ϕ, angle formed by the CPH plane and the normal to the HCH moiety) (Figure 5).

As expected, the minimum and maximum energies occur for ϕ equal to 90° and 0°, respectively; the corresponding barrier is equal to 300 kJ·mol^{-1}, while for the radical anion this barrier is only equal to 56 kJ·mol^{-1}. This drastic diminution of the barrier around the P=C bond is in accordance with the antibonding character of the orbital containing the unpaired electron.

ESR Spectra. 1. ESR Spectra of the Ligands. The radical anions were directly generated in the ESR cavity by imposing on the solution a voltage slightly lower (−100 mV) than that determined by cyclic voltametry. The same spectra (Figure 6a) were obtained with two solutions containing considerably different proportions of the EZ and EE isomers (solution 1, EE 95%, EZ 5%; solution 2, EZ 93%, EE 3.5%, ZZ 3.5%). Three patterns, marked A, B, and A' are clearly seen on this spectrum and are attributed to hyperfine interaction with two equivalent ^{31}P nuclei. While the ratio of intensities A/A' remains practically equal to unity, the ratio A/B is drastically dependent upon temperature; at room temperature, the ratio A/B is close to $^1/_2$ while at about 200 K the line width of the signal A is so large that only the B signal is observed. Additional ^{1}H hyperfine splittings could be detected on the B line by recording the spectrum at room temperature with a small modulation amplitude (Figure 6a). Due to the larger line width of the A and A' signals these extra couplings could not be resolved on these lines. In accord with the simulation (Figure 6b) this proton hyperfine structure corresponds to a triplet (14 MHz) of triplets (6 MHz) of doublets (3.3 MHz). Besides the phosphorus couplings, the spectra obtained at room temperature with a reduced solution of the deuterated compound, Ph(CD=PAr)$_2$, exhibited a well-resolved hyperfine structure with two equivalent protons (14 MHz). This proton structure was visible at the A, B, and A' positions (Figure 6c). It is therefore clear that the coupling constants of 6 MHz were caused by the two phosphaalkene protons, and the simulation of the liquid-phase spectra led, finally, to the following coupling constants for $\mathbf{L}^{\bullet-}$: 72 MHz (two ^{31}P nuclei), 14 MHz (two aromatic protons in positions 4 and 6), 6 MHz (two phosphaalkene protons) and 3.3 MHz (one aromatic proton in position 2 or 5). Probably due to line-broadening provoked by the unresolved deuterium coupling, the smallest splitting (3 MHz) could not be observed after deuteration of the phosphaalkene moieties.

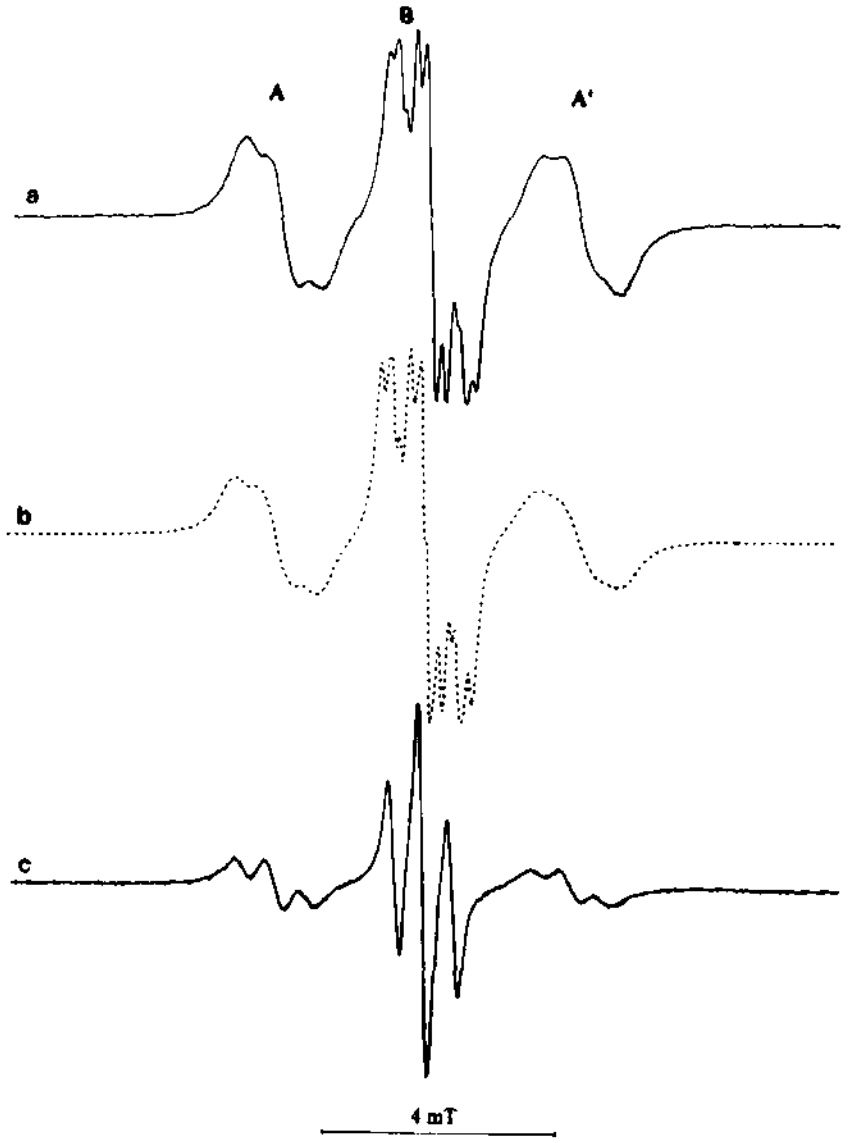

Figure 6. (a) ESR spectrum obtained with $\mathbf{L}^{\bullet-}$ in solution (THF) at room temperature. (b) Simulated spectrum (for this simulation the linewidth used for the A and A' lines is slightly larger than that used for the B lines). (c) Spectrum obtained with Ph(CD=PAr)$_2^{\bullet-}$.

The ESR spectrum obtained below 100 K with a frozen solution of $\mathbf{L}^{\bullet-}$ (Figure 7) is practically the same with the deuterated and the nondeuterated compound. Signals clearly appear at 328.2, 335.3, and 343.3 mT (ν = 9408 MHz) and undoubtedly result from phosphorus hyperfine interaction. For the analysis of this spectrum, it is reasonable to assume an axial hyperfine interaction with two equivalent ^{31}P nuclei whose

(34) (a) Pople, J. A.; Binkley, J. S.; Seeger, R. *Int. J. Quantum Chem. Symp.* **1976**, *10*, 1. (b) Krishnan, R.; Pople, J. A. *Int. J. Quantum Chem.* **1976**, *14*, 91).

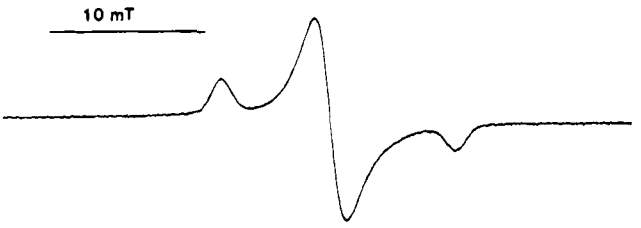

Figure 7. ESR spectrum obtained at 100 K with a frozen solution of L^- in THF.

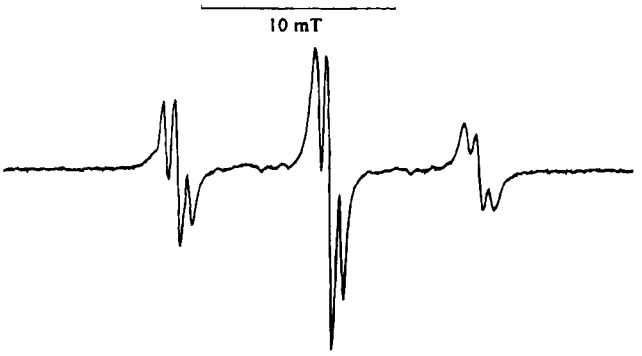

Figure 8. ESR spectrum obtained at room temperature with a solution of LPdNCMe in THF.

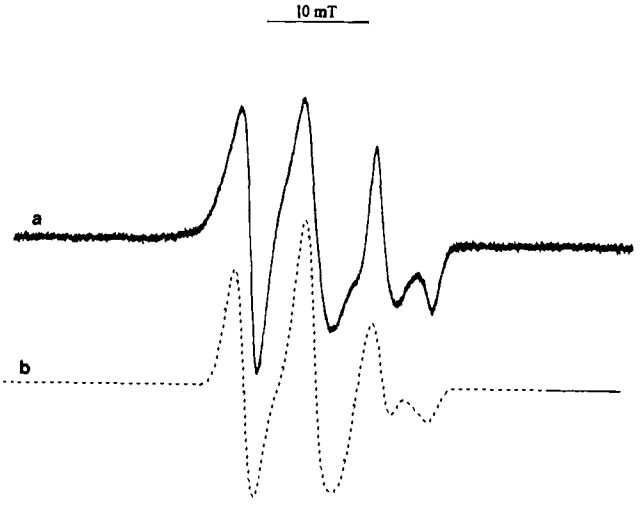

Figure 9. (a) ESR spectrum obtained with a frozen solution of $LPdCl^-$ in THF. (b) Simulated spectrum.

coupling tensors are aligned; the central line results from the overlap of the three perpendicular components ($m_I = 1, 0, -1$; $T_\perp$ is supposed to be small) and of the $m_I = 0$ component of the "parallel" subspectrum. This analysis leads to the following ^{31}P hyperfine tensor: $T_\parallel = 209$ MHz, $T_\perp = 3$ MHz.

2. ESR Spectra of the Complexes. A. Palladium Complexes. The ESR spectrum obtained after reduction of LPdCl is characterized by a coupling of 217 MHz with two ^{31}P nuclei and of 14 MHz with two ^1H. In contrast with the spectra recorded for the ligand, this spectrum is considerably less dependent upon temperature; in particular the relative intensities of the three sets of signals are almost constant between room temperature and 220 K. Moreover, the replacement of the phosphaalkene protons by deuterons shows that the coupling of 14 MHz is due to the protons of the CH=P groups. The solution ESR spectrum obtained with $LPdNCMe^+$ is very similar to the spectrum obtained with $LPdCl$[13] and is shown in Figure 8. In the frozen solution, at 100 K, both compounds lead to a spectrum (Figure 9a) which reflects a large anisotropy of the **g** tensor. The ESR parameters obtained after simulation (Figure 9b) are shown in Table 4. The isotropic coupling constants derived from these tensors are consistent with the values obtained in the liquid phase (see Table 4).

Table 4. ESR Eigenvalues[a] Obtained after Reduction of Metal Complexes of L[b]

complex		frozen solution			liquid
$LPdCl^-$	**g**	2.015	2.010	1.990	2.002
	^{31}P-**T**	188	188	240	217
	^1H (^2D)				14(2)
LPdNCMe	**g**	2.015	2.010	1.991	2.002
	^{31}P-**T**	190	190	220	217
	^1H				14
$LPtCl^-$	**g**	2.000	1.999	1.949	1.985
	^{31}P-**T**	90	87	162	110
	^{195}Pt-**T**	20	156	208	

[a] Eigenvalues of the hyperfine tensors **T** and isotropic coupling constants are given in MHz. [b] Solutions in THF.

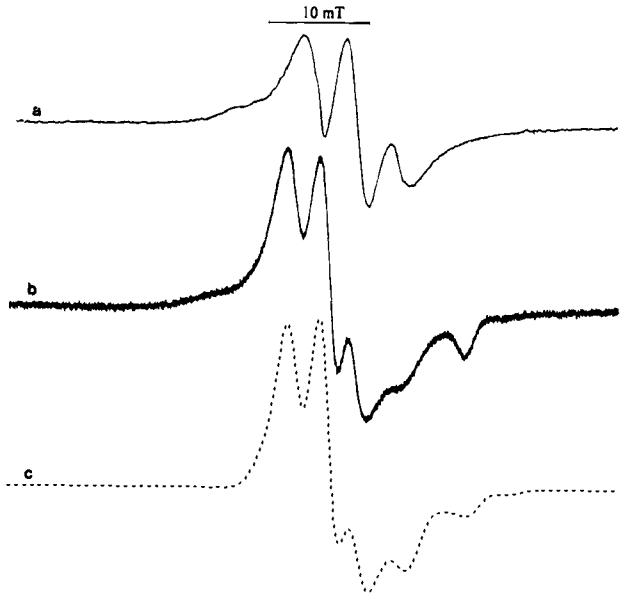

Figure 10. (a) Liquid solution (THF) spectrum of $LPtCl^-$. (b) Frozen solution of $LPtCl^-$ in THF. (c) Simulation of the frozen solution spectrum of $LPtCl^-$.

B. Platinum Complex. The large line width of the ESR signals obtained in solution with $(LPtCl)^-$ is probably due to unresolved hyperfine coupling with ^{195}Pt ($I = {}^1/_2$, natural abundance = 33.8%). Although this interaction considerably diminishes the resolution of the spectrum (Figure 10a), the splittings caused by two ^{31}P nuclei are clearly visible and correspond to a coupling of 110 MHz. The ESR spectrum obtained at 100 K for the frozen solution (Figure 10b) clearly exhibits a large anisotropy of the **g** tensor. An acceptable simulation was obtained (Figure 10c) by using the tensors (**g**, ^{195}Pt–**T**, two ^{31}P–**T**,) shown in Table 4. The **g** and ^{31}P coupling tensors are consistent with the average values observed in solution.

Discussion

Rotation Isomers for the Neutral Ligand. The fact that only three types of ^{31}P NMR spectra have been recorded with solutions of **L** indicates that rotation around the C(1)–C(7) and C(3)–C(8) bonds is free, and that this rotation prevents the distinction, for example, between E_1E_1 and E_1E_2. At room temperature, the presence of three isomers results, therefore, only from hindered rotation around the P=C bonds. This interpretation is consistent with *ab initio* calculations performed

Table 5. Calculated and Experimental Isotropic Coupling Constants[d] for $\mathbf{L'^-}$ and $\mathbf{L^-}$

	calculated averaged A_{iso} values for the C_{2v} rotamers of L'^{-} [a]	calculated A_{iso} values for the E_2E_2 rotamer of L'^{-} [b]	experimental[c] A_{iso} for $\mathbf{L^-}$
H(5)	0	0	0
H(4), H(6)	15.5	15.0	14
H(2)	0	0	3
H(7), H(8)	7.6	6.3	6
P(1), P(2)	50.0	62.6	72

[a] Calculations with the 6-31G* basis set. [b] Calculations with the 6-31++G** basis set. [c] Solutions in THF. [d] Values in MHz.

on $HP{=}CH_2$ which indicate that, even in the absence of any aromatic substituent, the rotation barrier around the P=C bond is close to 300 kJ·mol^{-1}. It is worthwhile noting that, as shown in Figure 2, X-ray structures indicate that in the crystal state, the EE isomer adopts the E_1E_1 conformation while the ZZ isomer adopts a distorted Z_1Z_2 structure. Unfortunately, the EZ isomer could not be crystallized.

Isomers for the Reduced Ligand. As shown by cyclic voltametry the one-electron reductions of solutions of EE and EZ occur at the same potential. The fact that the radical anions lead, in solution, to the same ESR spectrum regardless of the composition of the solution suggests that the rotation barriers around the C=P and $C_{phenyl}{-}C_{phosphaethylene}$ are so low that a rapid exchange occurs between the various isomers of $\mathbf{L^-}$ at room temperature. The broadening of the lines when cooling the electrolyzed solution is consistent with a "slowing" of this exchange with decreasing temperatures.

Keeping in mind that quantum chemistry predictions about the radical anion $\mathbf{L'^-}$ can only partially be representative of the structure of $\mathbf{L^-}$ (absence of steric interaction involving the Ar groups), we tried to use *ab initio* calculations to investigate to what extent the hyperfine structure was dependent upon the stereochemistry of the radical anion. However, as already mentioned, instabilities in the wave functions prevented us from calculating the hyperfine couplings for the rotamers of C_s symmetry, and only the isomers of C_{2v} symmetry could be investigated. As shown in Table 3, these latter isomers have similar spin populations, and the corresponding isotropic coupling constants could be roughly estimated by assuming that (1) the ^{1}H coupling is related to the C_α spin density through the McConnell constant[35] ($Q = -70$ MHz) and (2) ^{31}P coupling, mainly due to inner shell spin polarization, is proportional to the phosphorus 3pπ spin density with a coefficient close to 415 MHz.[36] A rapid exchange between the C_{2v} conformations leads to isotropic coupling constants which are shown in Table 5 together with the values obtained for the E_2E_2 isomer by using the 6.31^{++}G ** basis set. These coupling constants are rather close to the experimental values (Table 5). The dipolar ^{31}P coupling tensors were obtained from the phosphorus spin densities by using the atomic parameters calculated by Morton and Preston.[37] The resulting "powder" spectrum is characterized by a value of $2T_{\|}(^{31}P) \sim 12.3$ mT (splitting between the two external lines) while the corresponding experimental value (Figure 7) is equal to 15.2 mT. This difference is probably due, in part, to the contribution of the C_s structures which could not be taken into account for the calculations.

Complexes. While the ^{31}P NMR spectra show that for each Pd and Pt complex a single isomer exists in solution, the crystal structures indicate that, in each case, the diphosphaalkene ligand **L** adopts the E_1E_1 conformation and acts as a terdentate ligand; the metal is coordinated to two phosphorus atoms, and an orthometallation occurs. It is worthwhile mentioning that, as recently reported by Rüttiman *et al.*,[38] palladium does not give rise to 2-metallation with 1,3-(1-methylbenzimidazol-2-yl)-benzene, although this ligand contains two C=N bonds in *meta* position. As shown by the crystal structures, in the complexes of **L**, the two phosphaalkenes moieties, the central benzene ring, and the metal atom are perfectly coplanar. It can therefore be expected that after reduction, the additional electron can easily delocalize on both the metal and the ligand moieties.

As shown by cyclic voltametry (Table 2) the **LMX** complexes are easily reduced between -0.9 and -1.3 V, and the question is to know whether this process is based on the ligand or on the metal. For Ni, Pd, and Pt complexes, this problem has been mainly discussed in the case of sulfur ligands. For example, it was shown that reduction of the planar bis(dithio-β-diketonate)-nickel(II) is mainly a ligand-centered process[39] while for dithiocarbamates[40] and maleonitriledithiolates[41] the reduction was based on the metal. In the present case, the ESR spectra of the reduced LPdCl and $LPdNCMe^+$ species are characterized by a **g** value which is rather close to that of the free ligand. Their line widths, however, are considerably narrower than those observed for $\mathbf{L^{\bullet -}}$. The isotropic hyperfine constants observed with the palladium complexes (Table 4) are quite different from those observed in the absence of metal. In particular, the ^{1}H couplings, identified by deuteration, indicate that the unpaired electron is largely delocalized on each phosphaalkene carbon (*ca.* 20%). The fact that the ^{105}Pd coupling (^{105}Pd: $I = {}^5/_2$, natural abundance 22.2%) is not resolved suggests that, at least, the spin density on this atom is not preponderant. From the anisotropic coupling constants obtained after simulation of the frozen solution spectra (Table 4), it appears that the contribution of the p_π orbital of each phosphorus to the SOMO is *ca* 5%. Since the spin delocalization on the C(4)C(5)C(6) atoms of the phenyl group is rather small (since it does not give rise to any ^{1}H coupling in solution), a non-negligible fraction of the unpaired electron is probably delocalized on the metal ion. This is confirmed by the large anisotropy of the **g** tensor ($\mathbf{g}_{\|} < \mathbf{g}_\perp$) which reveals a participation of the metal orbitals in the SOMO.

The spectrum obtained with a liquid solution of LPtCl is also characterized by a triplet due to two equivalent ^{31}P nuclei, but the especially large line width precludes the observation of any additional structure. The small g value is in accord with the larger spin–orbit coupling constant of the platinum. Although the ^{31}P isotropic coupling is smaller than that found with the Pd compounds, the dipolar hyperfine tensors obtained from the frozen solution spectrum lead to a spin density in the p_π orbital of each phosphorus atom (6%) which is similar to that found for the palladium complexes. Moreover, for these latter compounds, the **g** tensor, characterized by $g_{\|} < g_\perp$, is reminiscent of previous results obtained with the few complexes in which the unpaired electron was localized in a ligand π^* molecular orbital. For example, reduction of stannic dichloride adducts of bis(dithiooxalato)nickelate(II), -palladate(II), and -platinate(II) complexes[42] led to ESR spectra whose hyperfine structure clearly indicated that the unpaired electron was mainly

(35) McConnell, H. M. *J. Chem. Phys.* **1956**, *25*, 890.
(36) Geoffroy, M.; Lucken, E. A. C.; Mazeline, C. *Mol. Phys.* **1974**, *28*, 839.
(37) Morton, J. R.; Preston, K. F. *J. Magn. Reson.* **1978**, *30*, 577.
(38) Rüttimann, S.; Bernardinelli, G.; Williams, A. F. *Angew. Chem., Int. Ed. Engl.* **1993**, *32*, 392.
(39) Bowmaker, G. A.; Boyd, P. D. W.; Zwagulis, M.; Cavell, K. J.; Masters, A. F. *Inorg. Chem.* **1985**, *24*, 401.
(40) Bowmaker, G. A.; Boyd, P. D. W.; Campbell, G. K.; Hope, J. M.; Martin, R. L. *Inorg. Chem.* **1982**, *21*, 1152.
(41) Geiger, W. E.; Allen, C. A.; Mines, T. E.; Senftleber, F. C. *Inorg. Chem.* **1977**, *16*, 2003.
(42) Bowmaker, G. A.; Boyd, P. D. W.; Campbell, G. K. *Inorg. Chem.* **1982**, *21*, 3565.

Table 6. ESR Parameters for Some Ligand-Centered Radical Anions

complex	ref	metal	g_1	g_2	g_3	metal coupling (MHz) T_1	T_2	T_3
$[M(S_2C_2O_2(SnCl_4)]^{3-}$ [a]	36	^{105}Pd	1.994	2.006	2.011	27	42	28
		^{195}Pt	1.973	2.011	2.016	−39	69	69
$[M(Ph_2C_2S_2)]^-$ [b]	37	^{105}Pd	1.960	2.041	2.051	15	20	27
		^{195}Pt	1.845	2.065	2.169	252	327	96
$[M(mnt)_2]^-$ [c]	35	^{105}Pd	1.956	2.044	2.070	16	19	27
$[M(tds)_2]^-$ [d]	38	^{195}Pt	1.820	2.143	2.230	225	270	70

[a] S_2C_2O: dithiooxalato. [b] PhC_2S_2: 1,2-diphenyl-1,2-ethenedithiolate. [c] mnt: maleonitrileedithiolate. [d] tds: [bis(trifluoromethyl)-ethylene]-diselenolato.

residing on the ligand. Similarly, the $[M(mnt)_2]^-$ complexes[41] (see Table 6 for definition of mnt) (with M = Ni, Pd) and the $[M(Ph_2C_2S_2)_2]^-$ complexes[43] (with M = Ni, Pd, Pt) exhibited proton hyperfine couplings in accord with the structure of ligand-centered radical anions. For these species, as well as for $[Pt(tds)_2]^-$,[44] (see Table 6 for definition of tds), the metal participates in the SOMO with its d_{yz} orbital which allows conjugation with the p_π orbitals of the ligands, and although the $g_{average}$ value is considerably closer to that of the free electron value than that with metal-centered complexes, the anisotropy of the **g** tensor is well marked (Table 6). In our case, the π direction, given by the ^{31}P eigenvectors, is indeed aligned along the $g_{||}$ direction and is perpendicular to the ^{195}Pt−T_{min} eigenvector (associated with the ^{195}Pt−$T_{||}$ direction in the axial approximation). The spin density on the Pt atom can been estimated from the equations of Maki *et al.*[45] for a d_{yz} ground state. Depending upon the relative signs of the ^{195}Pt, we obtain $\varrho(Pt) = 0.13$ or $\varrho(Pt) = 0.17$ which are quite consistent with the spin densities observed on the phosphaalkene moieties but which also suggest that the unpaired electron could be appreciably localized on the C(1)C(2)C(3) fragment.

(43) Bowmaker, G. A.; Boyd, P. D. W.; Campbell, G. K. *Inorg. Chem.* **1983**, *22*, 1208.

(44) Heuer, W. B.; True, A. E.; Swepston, P. N.; Hoffman, Brian. M. *Inorg. Chem.* **1988**, *27*, 1474.

Conclusion

NMR and crystal structures indicate that several rotamers exist for the novel benzodiphosphaalkene molecule, but ESR shows that free rotation around the P=C bonds probably occurs at room temperature after one-electron reduction. One of these rotamers acts as a terdentate ligand; it is orthometalated by Pd^{II} and Pt^{II} ions and coordinates the metal with its two phophorus atoms. The resulting complex is reversibly reduced to a paramagnetic species whose unpaired electron is mainly delocalized in a ligand π^* orbital. The presence of the metal is, however, clearly visible on the ESR spectrum of the frozen solution.

Acknowledgment. This work was supported by a grant from the Swiss National Research Fund. We thank Dr. Y. Ellinger for helpful discussions.

Supplementary Material Available: Table of atomic coordinates, displacement parameters, bond distances and bond angles, atomic numbering schemes (18 pages). This material is contained in many libraries on microfiche, immediately follows this article in the microfilm version of the journal, can be ordered from the ACS, and can be downloaded from the Internet; see any current masthead page for ordering information and Internet access instructions.

JA942012O

(45) Maki, A. H.; Edelstein, N.; Davison, A.; Holm, R. H. *J. Am. Chem. Soc.* **1964**, *86*, 4580. These equations of Maki *et al.* have been slightly modified by Heuer *et al.*[38]